Space vector modulation of nine-phase voltage source inverters based on three-phase decomposition

G. Grandi, G. Serra, A. Tani
UNIVERSITY OF BOLOGNA
Dept. of Electrical Engineering
Viale Risorgimento, 2 – Bologna Italy
Ph: +39 / 051 2093571, Fax: +39 / 051 2093588
URL: http://www.die.unibo.it

Abstract

A new space vector modulation (SVM) technique having a full and independent control of the multiple voltage space vectors of a nine-phase voltage source inverter (VSI) is presented in this paper. The proposed approach is based on the concept of system decomposition, leading to the modulation of three three-phase VSIs. The resulting SVM corresponds to standard SVM for each three-phase VSI in the case of a nine-phase load with three insulated central points, whereas the additional modulation of the zero-sequence component is introduced for each three-phase VSI in the case of a nine-phase load with a single central point. The modulation limits are investigated and the analytical developments are proved by a complete set of simulation results.

Introduction

Multi-phase motor drives have many advantages over the traditional three-phase motor drives such as reducing the amplitude and increasing the frequency of torque pulsations, reducing the rotor harmonic current losses and lowering the dc link current harmonics. In addition, owing to their redundant structure, multi-phase motor drives improve the system reliability. As a consequence, the use of multi-phase inverters together with multi-phase ac machines has been recognized as a viable approach to obtain high power ratings with current limited devices [1]-[4].

Among the various possible numbers of phases, the multiples of three present some advantages, such as the possibility to build the multi-phase inverter as a hardware combination of standard three-phase VSIs, having proved reliability and effective protection circuitry. Furthermore, the stator core laminations of the ac machine have a number of slots multiple of three, offering the possibility to realize the multi-phase stator core with minimum adjustment with respect to standard three-phase machines.

In alternative to the traditional carrier-based PWM, the multiple space vector approach can be adopted to determine the firing signals for the power switches of a multi-phase VSI, introducing the multi-phase space vector modulation (SVM) techniques [5], [6]. In fact, an extension of the well-known space vector theory can be still employed to represent the behaviour of multi-phase systems, leading to an elegant and effective vectorial approach in multiple *d-q* planes [7]. Nowadays, the modulation of nine-phase VSI has been discussed in [8], [9], [10]. However, a SVM algorithm for nine-phase VSI able to arbitrarily regulate all the multiple voltage space vectors has not been presented yet.

In this paper a new SVM technique for a nine-phase VSI is presented. The proposed three-phase decomposition leads to a triple three-phase system, opening the possibility to obtain a general SVM algorithm having a full and independent control of all the four voltage space vectors of the nine-phase VSI. In particular, it is shown that each one of the three-phase VSI can be regulated by a standard SVM technique only if the three central points of the triple three-phase load are insulated, whereas the modulation of the zero-sequence component must be introduced for each three-phase VSI in the case of a nine-phase load with a single central point.

 ISBN : 9789075815108

Space vector representation of nine-phase systems

Multiple Space Vector Transformation

The space vector transformation for a nine-phase system leads to a zero-sequence component and four opportune space vectors among the eight available ones [7], [8]. In this paper the following space vectors are adopted to represent the nine-phase system, being $\alpha = exp\,(j2\pi/9)$:

$$\begin{cases} x_0 = \frac{1}{9}\left[x_1 + x_2 + x_3 + x_4 + x_5 + x_6 + x_7 + x_8 + x_9\right] \\ \bar{x}_1 = \frac{2}{9}\left[x_1 + x_2\alpha + x_3\alpha^2 + x_4\alpha^3 + x_5\alpha^4 + x_6\alpha^5 + x_7\alpha^6 + x_8\alpha^7 + x_9\alpha^8\right] \\ \bar{x}_2 = \frac{2}{9}\left[x_1 + x_2\alpha^2 + x_3\alpha^4 + x_4\alpha^6 + x_5\alpha^8 + x_6\alpha + x_7\alpha^3 + x_8\alpha^5 + x_9\alpha^7\right] \\ \bar{x}_3 = \frac{2}{9}\left[\left(x_1 + x_4 + x_7\right) + \left(x_2 + x_5 + x_8\right)\alpha^3 + \left(x_3 + x_6 + x_9\right)\alpha^6\right] \\ \bar{x}_4 = \frac{2}{9}\left[x_1 + x_2\alpha^4 + x_3\alpha^8 + x_4\alpha^3 + x_5\alpha^7 + x_6\alpha^2 + x_7\alpha^6 + x_8\alpha + x_9\alpha^5\right] \end{cases} . \quad (1)$$

Note that the space vector $\bar{x}_3$ has a singular expression since 3 is a factor of the number of phases n = 9, which is not a prime. The resulting inverse transformation is

$$x_k = x_0 + \bar{x}_1 \cdot \alpha^{(k-1)} + \bar{x}_2 \cdot \alpha^{2(k-1)} + \bar{x}_3 \cdot \alpha^{3(k-1)} + \bar{x}_4 \cdot \alpha^{4(k-1)}, \qquad k = 1, 2, \ldots, 9 \quad (2)$$

where the symbol " $\cdot$ " denotes the inner (scalar) product. The four space vectors $\bar{x}_1$, $\bar{x}_2$, $\bar{x}_3$ and $\bar{x}_4$ lie in the planes called d_1-q_1, d_2-q_2, d_3-q_3, and d_4-q_4, respectively.

Three-phase space vector decomposition

The nine-phase system can be seen as the composition of three sub-systems $\{h\}$, h = 1, 2, 3, each of which having three phases, according to

$$\{1\}\begin{cases} x_1^{(1)} = x_1 \\ x_2^{(1)} = x_4 \\ x_3^{(1)} = x_7 \end{cases} \quad \{2\}\begin{cases} x_1^{(2)} = x_2 \\ x_2^{(2)} = x_5 \\ x_3^{(2)} = x_8 \end{cases} \quad \{3\}\begin{cases} x_1^{(3)} = x_3 \\ x_2^{(3)} = x_6 \\ x_3^{(3)} = x_9 \end{cases} . \quad (3)$$

The space vector $\bar{x}^{(h)}$ and the zero-sequence component $x_0^{(h)}$ can be defined for each sub-system $\{h\}$, leading to

$$\begin{cases} \bar{x}^{(h)} = \frac{2}{3}\left[x_1^{(h)} + x_2^{(h)}\alpha^3 + x_3^{(h)}\alpha^6\right] , \\ x_0^{(h)} = \frac{1}{3}\left[x_1^{(h)} + x_2^{(h)} + x_3^{(h)}\right] , \quad h = 1,\ 2,\ 3. \end{cases} \quad (4)$$

In this case, the resulting inverse transformation can be written as

$$x_k^{(h)} = x_0^{(h)} + \bar{x}^{(h)} \cdot \alpha^{3(k-1)}, \quad k, h = 1, 2, 3.$$

The relationship between the multiple space vectors of the nine-phase system and the three space vectors of the three-phase sub-systems is obtained by introducing (3) and (4) in (1), leading to

$$\begin{cases} x_0 = \dfrac{1}{3}\left[x_0^{(1)} + x_0^{(2)} + x_0^{(3)} \right] \\ \bar{x}_1 = \dfrac{1}{3}\left[\bar{x}^{(1)} + \bar{x}^{(2)}\alpha + \bar{x}^{(3)}\alpha^2 \right] \\ \bar{x}_2^* = \dfrac{1}{3}\left[\bar{x}^{(1)} + \bar{x}^{(2)}\alpha^{-2} + \bar{x}^{(3)}\alpha^{-4} \right] \\ \bar{x}_3 = \dfrac{2}{3}\left[x_0^{(1)} + x_0^{(2)}\alpha^3 + x_0^{(3)}\alpha^6 \right] \\ \bar{x}_4 = \dfrac{1}{3}\left[\bar{x}^{(1)} + \bar{x}^{(2)}\alpha^4 + \bar{x}^{(3)}\alpha^8 \right] \end{cases}. \tag{5}$$

The quantities x_0 and $\bar{x}_3$ in (5) are written as zero-sequence and space vector components, respectively, of the three zero-sequence components $x_0^{(h)}$ of the three-phase sub-systems. Then, the quantities $x_0^{(h)}$ are given by

$$x_0^{(h)} = x_0 + \bar{x}_3 \cdot \alpha^{3(h-1)}, \quad h = 1, 2, 3. \tag{6}$$

The space vectors $\bar{x}^{(h)}$ of the three-phase sub-systems can be expressed on the basis of the multiple space vectors $\bar{x}_1$, $\bar{x}_2^*$ (the complex conjugate of $\bar{x}_2$), and $\bar{x}_4$ as

$$\begin{cases} \bar{x}^{(1)} = \bar{x}_1 + \bar{x}_2^* + \bar{x}_4 \\ \bar{x}^{(2)} = \alpha^{-1}\bar{x}_1 + \alpha^2\bar{x}_2^* + \alpha^{-4}\bar{x}_4 \\ \bar{x}^{(3)} = \alpha^{-2}\bar{x}_1 + \alpha^4\bar{x}_2^* + \alpha^{-8}\bar{x}_4 \end{cases}. \tag{7}$$

Nine-phase VSI feeding a load with three insulated central points

The scheme of a 9-phase VSI feeding a balanced load connected as a triple three-phase system having three insulated central points $0^{(1)}$, $0^{(2)}$, $0^{(3)}$ is represented in Fig. 1.

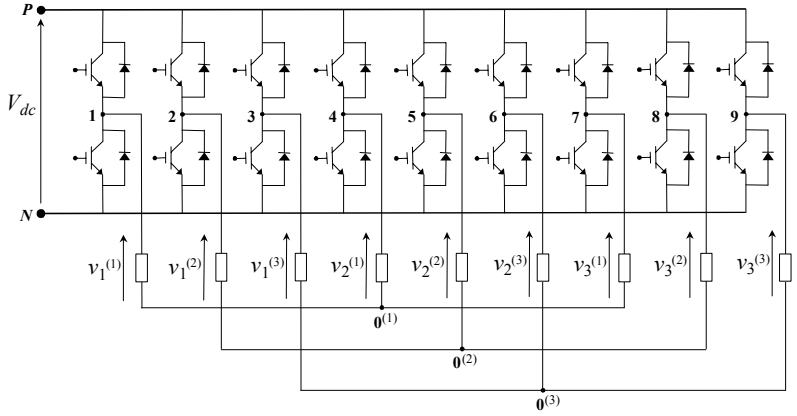

Fig. 1: Scheme of a nine-phase VSI feeding a nine-phase load with three insulated central points.

As shown in Fig. 1, the nine load voltages v_1, v_2, …, v_9 can be seen as the combination of the three voltages $v_1^{(h)}$, $v_2^{(h)}$, $v_3^{(h)}$ of the three three-phase sub-systems $\{h\}$, $h = 1, 2, 3$. In the same way, the nine-phase inverter can be seen as the combination of three standard three-phase VSIs connected to the same dc bus.

 ISBN : 9789075815108

Multiple space vectors of the load voltages

In the case of three insulated central points, both the zero-sequence component v_0 and the space vector $\bar{v}_3$ of the load voltages are always zero since in (5) the condition $v_0^{(h)} = 0$ applies for h = 1, 2, 3. The remaining space vectors can be written as

$$\begin{cases} \bar{v}_1 = \frac{2}{9} V_{dc} \left[S_1 + S_2\alpha + S_3\alpha^2 + S_4\alpha^3 + S_5\alpha^4 + S_6\alpha^5 + S_7\alpha^6 + S_8\alpha^7 + S_9\alpha^8 \right] \\ \bar{v}_2 = \frac{2}{9} V_{dc} \left[S_1 + S_2\alpha^2 + S_3\alpha^4 + S_4\alpha^6 + S_5\alpha^8 + S_6\alpha + S_7\alpha^3 + S_8\alpha^5 + S_9\alpha^7 \right] \\ \bar{v}_4 = \frac{2}{9} V_{dc} \left[S_1 + S_2\alpha^4 + S_3\alpha^8 + S_4\alpha^3 + S_5\alpha^7 + S_6\alpha^2 + S_7\alpha^6 + S_8\alpha + S_9\alpha^5 \right] \end{cases} . \quad (8)$$

There are 2^9 = 512 possible switch configurations. For space vectors 1, 2, and 4 (i.e., in d_1-q_1 , d_2-q_2, and d_4-q_4 planes), in addition to configurations (000000000) and (111111111) there are many other configurations corresponding to the null voltage vector. The remaining active configurations are represented by 342 different voltage vectors in each d-q plane, as depicted in Fig. 2.

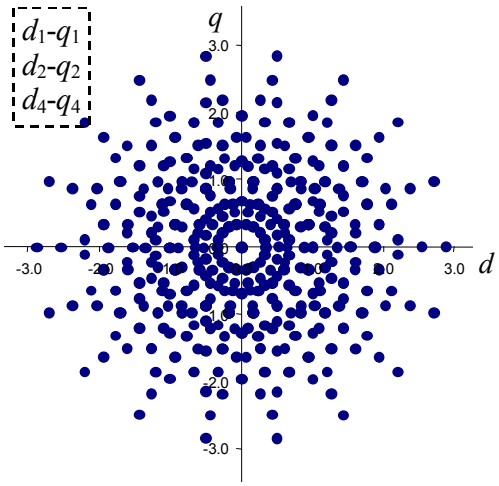

Fig. 2: Normalized voltage space vectors (with respect to 2/9 V_{dc}) of the nine-phase VSI.

Three-phase space vectors of the load voltages

As stated above, in the case of three insulated central points, the zero-sequence component for each sub-system $\{h\}$ is $v_0^{(h)} = 0$, leading to $\bar{v}_3 = 0$, whereas the space vector component of the load voltages can be written on the basis of (4) as

$$\bar{v}^{(h)} = \frac{2}{3} V_{dc} \left[S_1^{(h)} + S_2^{(h)}\alpha^3 + S_3^{(h)}\alpha^6 \right] , h = 1, 2, 3 . \quad (9)$$

The space vector $\bar{v}^{(h)}$ for each three-phase sub-system corresponds to the load voltage space vector of a standard three-phase VSI, as represented in Fig. 3. By combining (9) with (7) it is possible to determine the number of active voltage vectors as 7^3–1=342, as stated in the previous sub-section.

 ISBN : 9789075815108

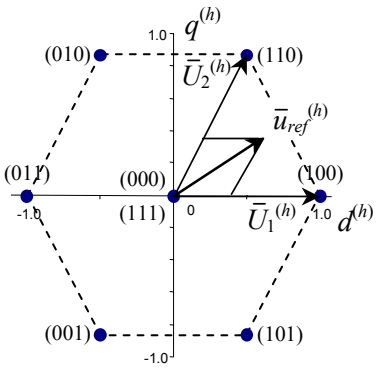

Fig. 3: Normalized voltage space vectors (with respect to 2/3 V_{dc}) for each three-phase VSI $\{h\}$.

Space vector modulation

The input variables for the SVM of the nine-phase VSI are usually represented by the references of multiple voltage space vectors $\bar{v}_{1ref}$, $\bar{v}_{2ref}$, and $\bar{v}_{4ref}$. The method proposed in this paper consists in determining the reference voltage space vector for each three-phase sub-systems $\{h\}$ by applying (7), leading to

$$\begin{cases} \bar{v}_{ref}^{(1)} = \bar{v}_{1ref} + \bar{v}_{2ref}^{*} + \bar{v}_{4ref} \\ \bar{v}_{ref}^{(2)} = \alpha^{-1}\bar{v}_{1ref} + \alpha^{2}\bar{v}_{2ref}^{*} + \alpha^{-4}\bar{v}_{4ref} \\ \bar{v}_{ref}^{(3)} = \alpha^{-2}\bar{v}_{1ref} + \alpha^{4}\bar{v}_{2ref}^{*} + \alpha^{-8}\bar{v}_{4ref} \end{cases}. \tag{10}$$

These space vectors can be independently synthesized by using the well-know three-phase SVM technique (Fig. 3). Then, duty-cycles $\delta_1^{(h)}$ and $\delta_2^{(h)}$ of the adjacent vectors $\bar{V}_1^{(h)}$ and $\bar{V}_2^{(h)}$ for each three-phase VSI are calculated by the following relationships:

$$\delta_1^{(h)} = \frac{\bar{v}_{ref}^{(h)} \cdot j\bar{V}_2^{(h)}}{\bar{V}_1^{(h)} \cdot j\bar{V}_2^{(h)}}, \quad \delta_2^{(h)} = \frac{\bar{v}_{ref}^{(h)} \cdot j\bar{V}_1^{(h)}}{\bar{V}_2^{(h)} \cdot j\bar{V}_1^{(h)}}, \quad h = 1, 2, 3. \tag{11}$$

Duty-cycles $\delta_0^{(h)}$ and $\delta_3^{(h)}$ of the null configurations (000) and (111) are determined to complete the switching period, according to

$$\delta_0^{(h)} + \delta_3^{(h)} = 1 - (\delta_1^{(h)} + \delta_2^{(h)}), \quad h = 1, 2, 3. \tag{12}$$

With reference to the three zero-sequence components $v_0^{(h)}$, they are all zero in the case of insulated central points, as stated above. In this case, the time-sharing between the null configurations is arbitrary, as for a standard three-phase VSI, leading to three degrees of freedom in the modulation process. In this case, the modulation process ends with (12).

Voltage limits

By considering a nine-phase load having three insulated central points, limits are determined for the voltage space vector $\bar{v}_1$, with reference to the condition: $\bar{v}_2 = 0$, $\bar{v}_3 = 0$, $\bar{v}_4 = 0$, as in the case of sinusoidal balanced voltages. In this case, (7) leads to the following voltage space vectors $\bar{v}^{(h)}$ for the three-phase VSIs:

$$\begin{cases} \bar{v}^{(1)} = \bar{v}_1 \\ \bar{v}^{(2)} = \alpha^{-1}\bar{v}_1 \\ \bar{v}^{(3)} = \alpha^{-2}\bar{v}_1 \end{cases}. \tag{13}$$

 ISBN : 9789075815108

Being the three three-phase VSIs independent one from the others, the voltage limits for each three-phase voltage space vector $\overline{v}^{(h)}$ are represented by the regular hexagon having the side 2/3 V_{dc}, as depicted in Fig. 3 (dashed line). On the basis of (13), the limits for the nine-phase voltage space vector $\overline{v}_1$ correspond to the 18-side regular polygon resulting from the intersection of three regular hexagons rotated by 0°, 20°, and 40°, respectively, as shown in Fig. 4. For sinusoidal balanced voltages, the voltage limits correspond to the inner circle having radius $V_{dc}/\sqrt{3}$ as represented by the shaded area in Fig. 4.

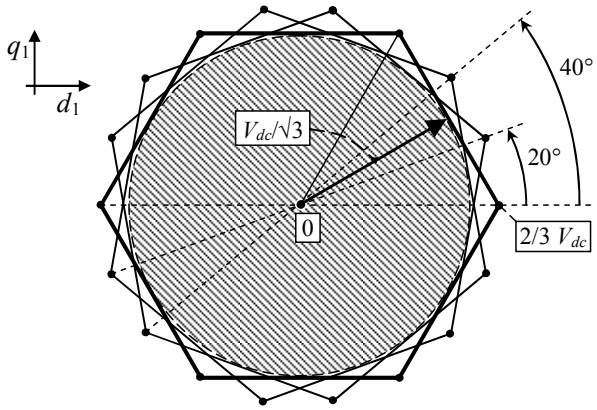

Fig. 4: Modulation limits for sinusoidal balanced voltages.

Nine-phase VSI feeding a load with a single central point

The scheme of a nine-phase VSI feeding a balanced load with a single central point 0 is represented in Fig. 5.

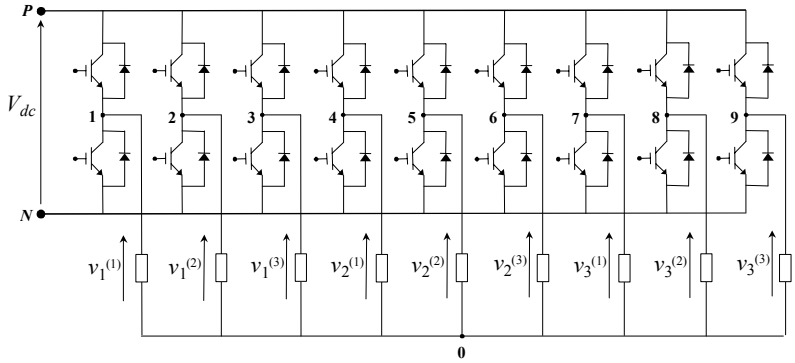

Fig. 5: Scheme of a nine-phase VSI feeding a load with a single central point.

Also in this case, the nine load voltages v_1, v_2, …, v_9 can be seen as the combination of the three voltages $v_1^{(h)}$, $v_2^{(h)}$, $v_3^{(h)}$ of the three three-phase sub-systems $\{h\}$, h = 1, 2, 3, as shown in Fig. 5. In the same way, the nine-phase inverter can be seen as the combination of three standard three-phase VSIs connected to the same dc bus.

Multiple space vectors of the load voltages

With reference to transformation (1), the zero-sequence component of the load voltages is always zero (balanced load), whereas the resulting four space vectors can be written as

 ISBN : 9789075815108

$$\begin{cases} \overline{v}_1 = \dfrac{2}{9}V_{dc}\left[S_1 + S_2\alpha + S_3\alpha^2 + S_4\alpha^3 + S_5\alpha^4 + S_6\alpha^5 + S_7\alpha^6 + S_8\alpha^7 + S_9\alpha^8\right] \\ \overline{v}_2 = \dfrac{2}{9}V_{dc}\left[S_1 + S_2\alpha^2 + S_3\alpha^4 + S_4\alpha^6 + S_5\alpha^8 + S_6\alpha + S_7\alpha^3 + S_8\alpha^5 + S_9\alpha^7\right] \\ \overline{v}_3 = \dfrac{2}{9}V_{dc}\left[(S_1 + S_4 + S_7) + (S_2 + S_5 + S_8)\alpha^3 + (S_3 + S_6 + S_9)\alpha^6\right] \\ \overline{v}_4 = \dfrac{2}{9}V_{dc}\left[S_1 + S_2\alpha^4 + S_3\alpha^8 + S_4\alpha^3 + S_5\alpha^7 + S_6\alpha^2 + S_7\alpha^6 + S_8\alpha + S_9\alpha^5\right] \end{cases} . \quad (14)$$

For space vectors 1, 2, and 4 (i.e., in d_1-q_1 , d_2-q_2, and d_4-q_4 planes), the considerations are the same as in the previous case of three insulated central points, as represented in Fig. 6(a). For space vector 3 (i.e., in the d_3-q_3 plane) there are many configurations corresponding to the null vector and many configurations corresponding to each one of the 36 active vectors, as represented in Fig. 6(b).

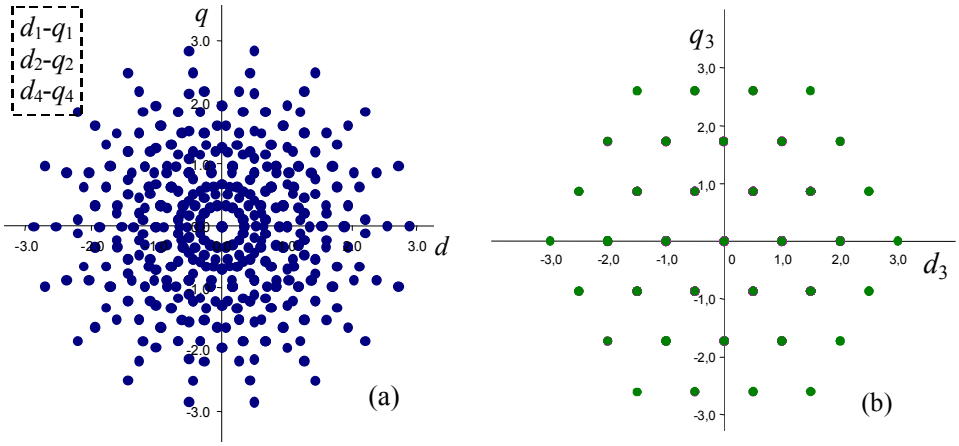

Fig. 6: Normalized multiple voltage space vectors (with respect to 2/9 V_{dc}) of the nine-phase VSI.

Three-phase space vectors of the load voltages

By applying the three-phase decomposition (4), space vector and zero-sequence components of load voltages for each three-phase sub-system $\{h\}$ can be written as

$$\overline{v}^{(h)} = \frac{2}{3}V_{dc}\left[S_1^{(h)} + S_2^{(h)}\alpha^3 + S_3^{(h)}\alpha^6\right], \; h = 1, 2, 3 \quad (15)$$

$$v_0^{(h)} = \frac{1}{3}V_{dc}\left[S_1^{(h)} + S_2^{(h)} + S_3^{(h)} - \frac{1}{3}\sum_{k=1}^{9} S_k\right], \; h = 1, 2, 3 . \quad (16)$$

As in the previous case of three insulated central points, voltage space vector $\overline{v}^{(h)}$ for each three-phase sub-system corresponds to voltage space vector of a standard three-phase VSI, as represented in Fig. 7(a). In this case, with a single central point, zero-sequence components of load voltages $\{v_0^{(h)}\}$ are generally different from zero, as expressed by (15), leading to the scalar diagram of Fig. 7(b).

Space vector modulation

With reference to the desired voltage space vectors $\overline{v}_{1ref}$, $\overline{v}_{2ref}$, and $\overline{v}_{4ref}$, the modulation procedure is based on (10) and (11), as in the previous case of three insulated central points. However, in case of a single central point, the additional voltage space vector $\overline{v}_{3ref}$ must be considered, leading to values of $v_{0ref}^{(h)}$ that are generally different from zero, as depicted in Fig. 7(b). By applying (6) yields

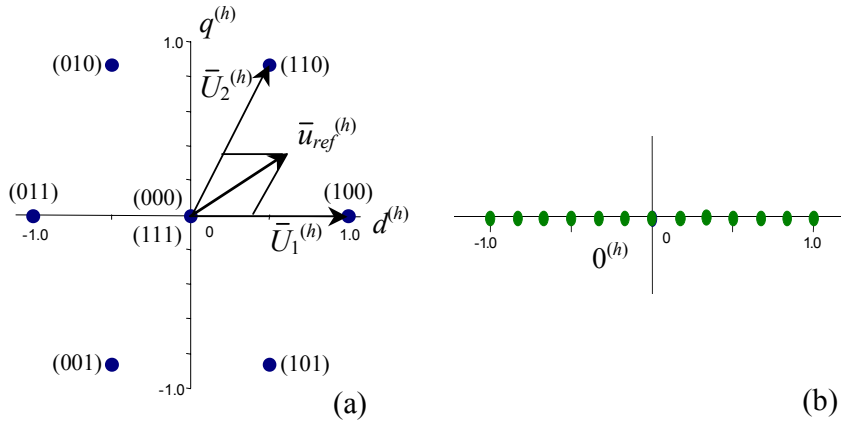

Fig. 7: Normalized voltage diagrams (with respect to 2/3 V_{dc}) for each three-phase VSI $\{h\}$: (a) space vector, (b) zero-sequence component.

$$v_{0ref}^{(h)} = \bar{v}_{3ref} \cdot \alpha^{3(h-1)}, \quad h = 1, 2, 3. \tag{17}$$

In this case, (12) still applies but a proper time-sharing between the two null configurations (000) and (111) must be determined for each three-phase inverter $\{h\}$. For this purpose, the relationship between the duty-cycles and $\bar{v}_{3ref}$ is derived from (14) leading to

$$\bar{v}_{3ref} = \frac{2}{9} V_{dc} \sum_{h=1}^{3} \left(\delta_1^{(h)} + 2\delta_2^{(h)} + 3\delta_3^{(h)} \right) \alpha^{3(h-1)}. \tag{18}$$

Note that duty-cycles $\delta_1^{(h)}$ and $\delta_2^{(h)}$ are determined by (11) on the basis of $\bar{v}_{1ref}$, $\bar{v}_{2ref}$, and $\bar{v}_{4ref}$, whereas duty-cycles $\delta_3^{(h)}$ must be determined to satisfy the desired voltage space vector $\bar{v}_{3ref}$, as expressed by (18). Introducing the auxiliary space vector $\bar{\delta}_3$ of the duty-cycle $\delta_3^{(h)}$

$$\bar{\delta}_3 = \frac{2}{3} \left(\delta_3^{(1)} + \delta_3^{(2)} \alpha^3 + \delta_3^{(3)} \alpha^6 \right), \tag{19}$$

(18) leads to

$$\bar{\delta}_3 = \frac{1}{V_{dc}} \bar{v}_{3ref} - \frac{2}{9} \sum_{h=1}^{3} \left(\delta_1^{(h)} + 2\delta_2^{(h)} \right) \alpha^{3(h-1)}. \tag{20}$$

Eq. (20) does not allow determining $\delta_3^{(1)}$, $\delta_3^{(2)}$, $\delta_3^{(3)}$ univocally. Introducing as a further scalar constraint their average value δ_3^o (i.e., their zero-sequence component)

$$\delta_3^o = \frac{1}{3} \left(\delta_3^{(1)} + \delta_3^{(2)} + \delta_3^{(3)} \right), \tag{21}$$

the solution can be written in the following parametric form

$$\delta_3^{(h)} = \bar{\delta}_3 \cdot \alpha^{3(h-1)} + \delta_3^o \quad , \quad h = 1, 2, 3. \tag{22}$$

Note that the value of arbitrary parameter δ_3^o does not affect the average value of the load voltages within the switching period, representing a single degree of freedom in the modulation process, compared to the three degrees of freedom expressed by (12) in the case of insulated central points. The modulation process ends with the determination of duty cycles $\delta_0^{(h)}$ as

$$\delta_0^{(h)} = 1 - \delta_1^{(h)} - \delta_2^{(h)} - \delta_3^{(h)}, \quad h = 1, 2, 3. \tag{23}$$

 ISBN : 9789075815108

Voltage limits

In the case of a nine-phase load having a single central point, the approach for determining the modulation limits is different with respect to the case of a load with three insulated central points. In fact, in this case, the modulations of the three three-phase VSI are not independent one from the others, due to the additional relationship (17) that must be satisfied to fix the value of $\overline{v}_{3ref}$. The coupling among the three three-phase VSIs is emphasized by (16), showing that the state of a single leg S_k affects the values of all the three zero-sequence components $v_0^{(h)}$.

The general approach to determine the modulation limits consists in introducing the non-negative constraint for all the duty cycles. Being $\delta_1^{(h)}$ and $\delta_2^{(h)}$ non-negative by definition, as expressed by (11) and Fig. 3, the remaining conditions to be satisfied are represented by

$$\delta_0^{(h)} \geq 0,\ \delta_3^{(h)} \geq 0\ , \quad h = 1, 2, 3. \tag{24}$$

Introducing (22) in (24) leads to

$$-min\{\overline{\delta}_3 \cdot \alpha^{3(h-1)},\ h=1,2,3\} \leq \delta_3^{o} \leq 1-max\{\delta_1^{(h)} + \delta_2^{(h)} + \overline{\delta}_3 \cdot \alpha^{3(h-1)}, h=1,2,3\}. \tag{25}$$

Eq. (25) specifies the validity domain of δ_3^{o}. As a consequence, the modulation constraints can be expressed as follows

$$-min\{\overline{\delta}_3 \cdot \alpha^{3(h-1)},\ h=1,2,3\} \leq 1-max\{\delta_1^{(h)} + \delta_2^{(h)} + \overline{\delta}_3 \cdot \alpha^{3(h-1)}, h=1,2,3\}. \tag{26}$$

The voltage limits can be obtained by introducing (11) and (20) in (26). By considering a nine-phase load having a single central point, limits are determined for the voltage space vector $\overline{v}_1$, with reference to the condition: $\overline{v}_2 = 0,\ \overline{v}_3 = 0,\ \overline{v}_4 = 0$. It can be shown that space vector $\overline{v}_1$ is limited by a 18-side regular polygon having radius $V_{dc}/[2cos^2(\pi/18)]$. For sinusoidal balanced voltages, the voltage limits correspond to the inner circle having radius $V_{dc}/[2cos(\pi/18)] \cong 0.508\ V_{dc}$, in agreement with [8].

Analysis of the switching pattern

In order to emphasize the relationship between the nine-phase SVM and the SVM obtained by the proposed three-phase decomposition, an example of switching pattern is shown in Table I. Reference is made to the space vectors depicted in Fig. 8 (nine-phase) and Fig. 9 (triple three-phase). Table I clearly shows that $\delta_0 = min\{\delta_0^{(h)}\}$ and $\delta_9 = min\{\delta_3^{(h)}\}$.

Discontinuous switching mode is obtained by selecting either $\delta_0 = 0$ or $\delta_9 = 0$ (the state of one leg remains unchanged within the switching period). On the basis of (22) and (23), these conditions are given by $\delta_3^{o} = 1 - max\{\delta_1^{(h)} + \delta_2^{(h)} + \overline{\delta}_3 \cdot \alpha^{3(h-1)}\}$ and $\delta_3^{o} = -min\{\overline{\delta}_3 \cdot \alpha^{3(h-1)}\}$, respectively. The symmetric modulating condition $\delta_0 = \delta_9$ is obtained when $min\{\delta_0^{(h)}\} = min\{\delta_3^{(h)}\}$.

Simulation results

In order to verify the effectiveness of the proposed SVM strategy, the behaviour of a system consisting of a nine-phase VSI feeding a nine-phase balanced R-L load with a single central point has been tested by numerical simulations ($R = 20\ \Omega$, $L = 10$ mH, $V_{dc} = 540$ V, see Fig. 5).

 ISBN : 9789075815108

Table I: SVM for the three-phase sub-systems and resulting nine-phase switching pattern

sub-system {1}		sub-system {2}		sub-system {3}		nine-phase system	
duty-cycle	$S_1S_4S_7$	duty-cycle	$S_2S_5S_8$	duty-cycle	$S_3S_6S_9$	duty-cycle	$S_1S_2S_3S_4S_5S_6S_7S_8S_9$
$\delta_0^{(1)}$	000	$\delta_0^{(2)}$	000	$\delta_0^{(3)}$	000	δ_0	000000000
$\delta_1^{(1)}$	100		000		000	δ_1	100000000
	100	$\delta_1^{(2)}$	100		000	δ_2	110000000
	100		100	$\delta_1^{(3)}$	001	δ_3	110000001
	100		100	$\delta_2^{(3)}$	101	δ_4	111000001
	100	$\delta_2^{(2)}$	101		101	δ_5	111000011
$\delta_2^{(1)}$	110		101		101	δ_6	111100011
$\delta_3^{(1)}$	111		101		101	δ_7	111100111
	111	$\delta_3^{(2)}$	111		101	δ_8	111110111
	111		111	$\delta_3^{(3)}$	111	δ_9	111111111

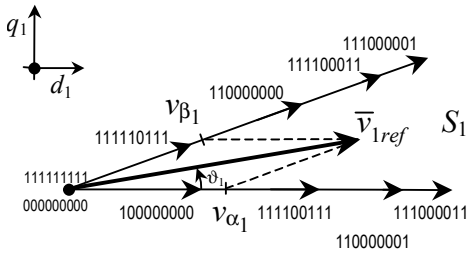

Fig. 8: SVM corresponding to switching pattern of Table I for the nine-phase VSI.

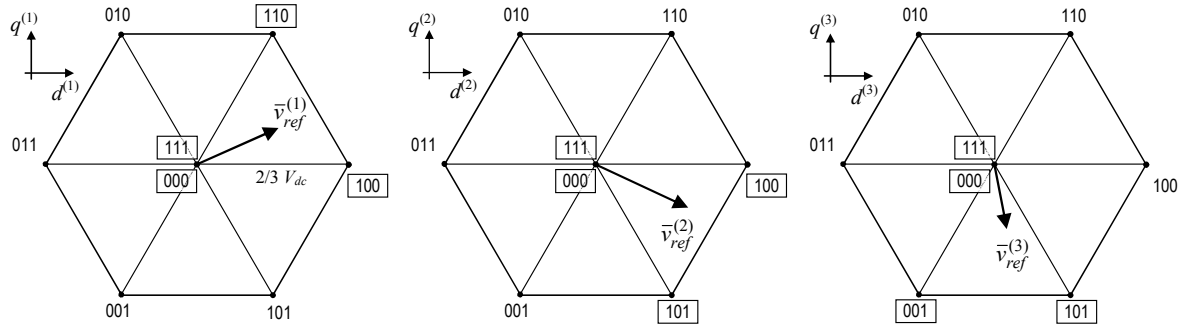

Fig. 9: SVM corresponding to switching pattern of Table I for the three three-phase VSIs.

The choice $\delta_0 = \delta_9$ (see Table I) has been considered for the null configurations in each switching period (T = 200 μs). The resulting SVM strategy can be considered as an extension of the well-known "symmetrical SVM" utilized for the three-phase VSI.

First of all, the behaviour of the system is analyzed in balanced and sinusoidal conditions (case A), with an amplitude of the reference load voltage $|\overline{v}_{1ref}|$ = 274 V, corresponding to the voltage limit [8] (V_{dc} = 540 V, m = 0.508), and a frequency of 50 Hz. In this case, $|\overline{v}_{2ref}|$, $|\overline{v}_{3ref}|$, and $|\overline{v}_{4ref}|$ are set to zero. The results of the numerical simulations are shown in Figs. 10-12.

The line-to-neutral load voltage v_1 is represented in Fig. 10a, showing a 17-levels waveform: $0, \pm\frac{1}{9}V_{dc}, \pm\frac{2}{9}V_{dc}, ..., \pm\frac{8}{9}V_{dc}$. In particular, the instantaneous value of v_1 changes across nine adjacent levels in a voltage range of $\frac{8}{9}V_{dc}$ within each switching period [8].

The nine load currents are shown in Fig. 10b. As expected, the waveforms are practically sinusoidal and characterized by a small ripple due to the switching effect.

In Fig. 11 are illustrated the trajectories of the space vectors $\overline{i}_1$, $\overline{i}_2$, $\overline{i}_3$, and $\overline{i}_4$ in the corresponding *d-q* planes. As expected, the space vectors $\overline{i}_2$, $\overline{i}_3$, and $\overline{i}_4$ are practically null, whereas $\overline{i}_1$ moves along a circular trajectory (at constant speed).

The spectrum of the load current shown in Fig. 12 confirms the effectiveness of the proposed modulation strategy, emphasizing the switching harmonics (around 5 kHz) and the fundamental component (50 Hz).

 ISBN : 9789075815108

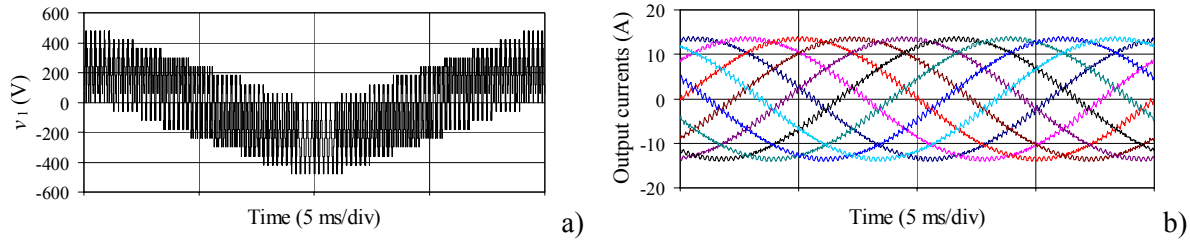

Fig. 10: Line-to-neutral load voltage waveform a) and load current waveforms b) (Case A).

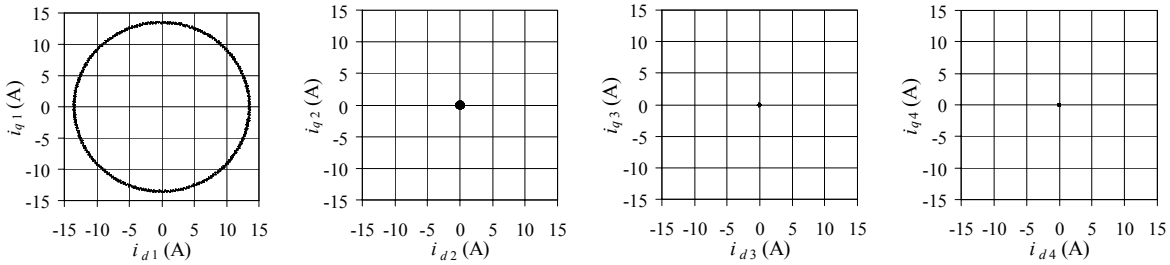

Fig. 11: Trajectories of space vectors $\bar{i}_1$, $\bar{i}_2$, $\bar{i}_3$, and $\bar{i}_4$ in the corresponding *d-q* planes (Case A).

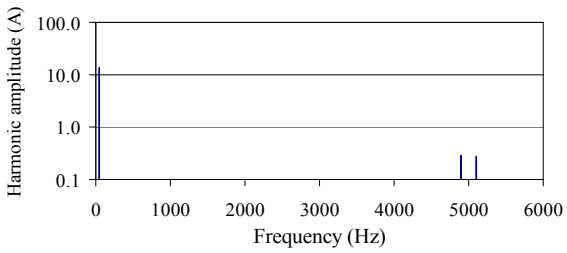

Fig. 12: Spectrum of the load current (Case A).

The second operating condition considered (case B) is characterized by four voltage space vectors different from zero, having the same constant amplitude ($|\bar{v}_{1ref}|=|\bar{v}_{2ref}|=|\bar{v}_{3ref}|=|\bar{v}_{4ref}|$=80 V), and rotating counter clockwise with angular frequency $\omega_1=2\pi$ 50 rad/s, $\omega_2=2\pi$ 350 rad/s, $\omega_3=2\pi$ 150 rad/s, and $\omega_4=2\pi$ 250 rad/s. The results of the numerical simulations are shown in Figs. 13-15.

The line-to-neutral load voltage v_1 is illustrated in Fig. 13a, whereas the non sinusoidal waveform of load current i_1 is shown in Fig. 13b. For the sake of readability, only load current i_1 is shown, being the other current waveforms identical and displaced by $2\pi/9$ one from the others.

In Fig. 14 are illustrated the trajectories of the space vectors $\bar{i}_1$, $\bar{i}_2$, $\bar{i}_3$, and $\bar{i}_4$ in the corresponding *d-q* planes. As expected, all four current space vectors move along a circular trajectory.

The spectrum of the load current, in the low frequency range, is shown in Fig. 15. The expected harmonic components, with decreasing amplitude, are clearly recognizable.

These results demonstrate that the proposed SVM strategy is able to independently control the output voltage space vectors in the four different *d-q* planes.

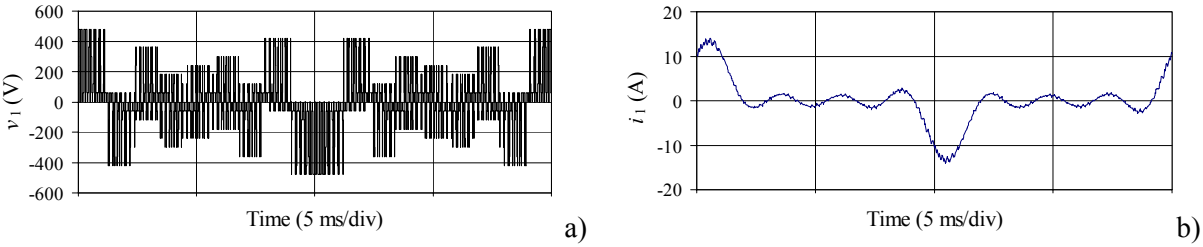

Fig. 13: Line-to-neutral load voltage waveform a) and load current waveform b) (Case B).

 ISBN : 9789075815108

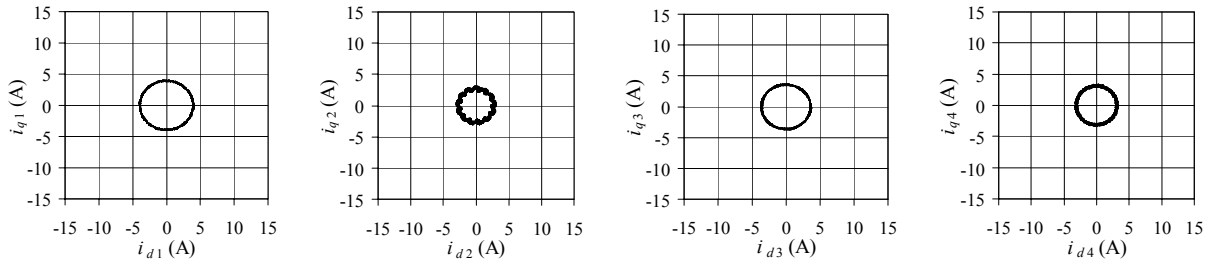

Fig. 14: Trajectories of space vectors $\bar{i}_1$, $\bar{i}_2$, $\bar{i}_3$, and $\bar{i}_4$ in the corresponding *d-q* planes (Case B).

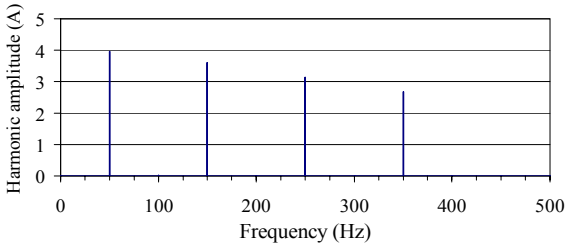

Fig. 15: Spectrum of the load current (Case B).

Conclusion

This paper shows that is possible to regard the SVM of a nine-phase VSI as the combination of the SVM of three three-phase VSIs. The proposed approach leads to a general modulation technique with a full and independent regulation of all the four voltage space vectors of the nine-phase VSI in both the cases of three insulated central points and single central point for the nine-phase load. The modulation limits are investigated and the analytical developments are proved by a complete set of simulation results. The proposed method can be easily extended to any odd number of phases multiple of three.

References

[1] H.A. Toliyat, S.P. Waikar, T.A. Lipo: Analysis and simulation of five-phase synchronous reluctance machines including third harmonic of airgap MMF, IEEE Trans. on IA, vol. 34, no. 2, Mar/Apr 1998.

[2] H. Xu, H.A. Toliyat, L.J. Petersen: Five-phase induction motor drives with DSP-based control system, IEEE Trans. on Power Electronics, vol. 17, No. 4, pp. 524-533, July 2002.

[3] M. Jones and E. Levi: A literature survey of state-of-the-art in multiphase AC drives, Proc. 37th Int. Universities Power Engineering Conf. UPEC, Stafford, UK, pp. 505-510, 2002.

[4] G.K. Singh: Multi-phase induction machine drive research – a survey, Electric Power Systems Research, vol. 61, no. 2, pp. 139-147, 2002.

[5] H.M. Ryu, J.H.Kim, S.K. Sul: Analysis of Multiphase Space Vector Pulse-Width Modulation Based on Multiple d-q Spaces Concept, IEEE Trans. on Power Electronics, Vol. 20, No. 6, November 2005.

[6] G. Grandi, G. Serra, A. Tani: Space Vector Modulation of a Seven-Phase Voltage Source Inverter, Proc. of SPEEDAM 2006, Taormina (Italy), May 23-26, 2006.

[7] Grandi, G. Serra, A. Tani: General analysis of multi-phase systems based on space vector approach, Proc. of EPE-PEMC, Portoroz (Slo), Aug. 30 - Sept. 1, 2006.

[8] G. Grandi, G. Serra, A.Tani: Space vector modulation of a nine-phase voltage source inverter, IEEE International Symposium on Industrial Electronics, IEEE-ISIE, Vigo (Spain), June 4-7, 2007.

[9] J.W. Kelly, E.G. Strangas, J.M. Miller: Multiphase space vector Pulse Width Modulation, IEEE Trans. on Energy Convers., vol. 18, no. 2, pp. 259-264, June 2003.

[10] C.E. Coates, D. Platt, V.J. Gosbell: Performance Evaluation of a Nine-phase Synchronous Reluctance Drive, 36th IEEE-IAS Annual Meeting, 30 Sept.-4 Oct. 2001, Vol. 3, pp. 2041 – 2047.